Giant enhancement of *n*-type carrier mobility in highly strained germanium nanostructures

F. Murphy-Armando,[1,a)] and S. Fahy[2]
[1]*Tyndall National Institute, University College, Cork, Ireland*
[2]*Department of Physics, University College, Cork, Ireland*

(Received 15 February 2011; accepted 12 April 2011; published online 2 June 2011)

First-principles electronic structure methods are used to predict the rate of *n*-type carrier scattering due to phonons in highly-strained Ge. We show that strains achievable in nanoscale structures, where Ge becomes a direct bandgap semiconductor, cause the phonon-limited mobility to be enhanced by hundreds of times that of unstrained Ge, and over a thousand times that of Si. This makes highly tensile strained Ge a most promising material for the construction of channels in CMOS devices, as well as for Si-based photonic applications. Biaxial (001) strain achieves mobility enhancements of 100 to 1000 with strains over 2%. Low temperature mobility can be increased by even larger factors. Second order terms in the deformation potential of the Γ valley are found to be important in this mobility enhancement. Although they are modified by shifts in the conduction band valleys, which are caused by carrier quantum confinement, these mobility enhancements persist in strained nanostructures down to sizes of 20 nm. © *2011 American Institute of Physics*. [doi:10.1063/1.3590334]

I. INTRODUCTION

Increasing the carrier mobility is key to both improving the performance and reducing the power dissipation in CMOS technology devices.[1] Historically, a gradual increase in mobility has been obtained by reducing the size of the carrier channels, and later by the strain engineering of Si. More recently, the search has also focused on incorporating other materials with a mobility higher than that of Si in the channel. This has proved to be a difficult task, since materials that are compatible with the established Si-fabrication technologies are hard to obtain. One of the few materials that can fulfill these two conditions is Ge. The mobility of Ge is two to three times higher than that of Si, and even more if slightly strained. Further interest in strained Ge has been stimulated by the recent accomplishment of lasing,[2] which makes the integration of photonic devices and lasers compatible with the Si fabrication process possible.

Previous studies[3,4] have suggested the possibility of enhancing the mobility of tensile strained Ge a few times further by turning it into a direct gap semiconductor. This is predicted to occur at 2% biaxial (001)[3,5] and 4% uniaxial $\langle 111 \rangle$[5,6] strains, among others. While these strains are unsustainable in bulk material due to the growth of strain-relieving dislocations, they are readily achieved in nanoscale structures with dimensions less than the critical thickness. The first type of strain has recently been achieved on thin films of Ge grown on $In_x Ga_{1-x}As$ substrates,[7] where direct gap photoluminesence has been observed. Strains of the second type have been experimentally surpassed in nanowires,[8,9] where strains up to 17% have been achieved.

In this work, we use recently developed[10] methods for calculating electron-phonon transport parameters from first principles to predict an enhancement of the *n*-type mobility of tensile strained Ge of ten to a thousand times that of unstrained Ge, which is over two orders of magnitude larger than previously estimated.[3,4] Extremely high mobilities such as these would dramatically increase the operational speed while significantly reducing the power dissipation of CMOS devices, two critical factors for the further advancement of this technology.

We calculate the mobility of Ge stressed in two different configurations: uni-axially along the $\langle 111 \rangle$ direction, and bi-axially on the (001) plane. Although some parameters are already available from experiments and empirical pseudopotential methods, using first principles calculations we corroborate the required energy splittings and phonon deformation potentials at small strains and calculate them as functions of strain for higher strain values. We then use the Boltzmann transport equation in the relaxation time approximation to obtain the *n*-type carrier mobility as a function of strain. We predict very significant increases in room temperature mobility for uni- and bi-axial strains larger than 1.5%, and increases of one to two orders of magnitude for strains greater than 2%. We also consider the effect on the mobility of reducing the channel size, and find that the mobility enhancement diminishes for channel sizes below 20 nm, due to the stronger quantum confinement of the Γ band compared to the *L* band.

II. THEORY AND METHOD

We can roughly estimate the expected enhancement of the mobility, obtained by confining electron transport to the Γ valley, by considering a parabolic approximation for the Γ and *L* valleys. Assuming the scattering to be isotropic, the ratio of mobilities is then[3]

a)Author to whom correspondence should be addressed. Electronic mail: philip.murphy@tyndall.ie

$$\frac{\mu_\Gamma}{\mu_L} = \frac{\langle \tau_\Gamma \rangle}{\langle \tau_L \rangle} \frac{m_c^L}{m^\Gamma} = \frac{\Xi_L^2 \left(m_d^L\right)^{3/2}}{\Xi_\Gamma^2 \left(m_d^\Gamma\right)^{3/2}} \frac{m_c^L}{m^\Gamma}, \quad (1)$$

where μ_i, with $i = L$ or Γ, is the mobility of the L or Γ valley, $\langle \tau_i \rangle$ is the thermal average of the relaxation time and the conduction masses are $m_c^L = 0.12 m_e$ and $m^\Gamma = 0.04 m_e$[3,11] for the L and Γ valleys, respectively, and m_e is the free electron mass. The effective deformation potential for the L valley is $\Xi_L = 11.5$ eV, calculated from Eq. (28) of Ref. 3, using the values of Ξ_u and Ξ_d of Ref. 10. The deformation potential for the Γ valley is $\Xi_\Gamma = -5.3$eV, and m_d^i is the density of states effective mass of valley i, with $m_d^L = 0.23 m_e$, and $m_d^\Gamma = m^\Gamma$. Thus, the enhancement expected by isolating the Γ valley will be on the order of $\mu_\Gamma / \mu_L = 182$. However, this spectacular enhancement can only be achieved if the zone center valley is well below the larger density of states L valley. Also, one has to consider how the deformation potential and effective mass of the Γ valley change at large applied strains. Without yet resorting to the full scale calculation, we can estimate the result of these considerations by using the calculated dependence of the Ξ_Γ deformation potential and of the m_Γ mass (discussed below), and multiplying the r.h.s. of Eq. (1) by the ratio of the carrier occupations n_Γ / n_L of the Γ and L valleys. This results in, for example, a 40 times enhancement for the 5% $\langle 111 \rangle$ uniaxial strain, and 500 times for the 2.5% (001) biaxial strain. We consider all these effects below, and demonstrate that the mobility enhancement can be as high as this crude estimate.

From what we have discussed above, it is clear that the possibility of enhancing the mobility in strained Ge is determined by the following competing effects:

- Avoiding a closure of the bandgap, where Ge becomes a semimetal,
- lowering of the Γ valley below the L valleys,
- decreasing the effective mass of the Γ valley due to the decreasing direct bandgap,
- nonlinearities in the Γ valley deformation potential, which may change the magnitude of the acoustic-phonon scattering.

The Γ valley has to be sufficiently far below the L valleys so that there are enough carriers in the former valley to dominate conduction. The decreasing effective mass will substantially enhance mobility, but also decreases the density of states of the Γ valley, thus in turn, requiring it to be much lower in energy than the L valley if the majority of carriers are to populate the Γ valley. At the strains in which this occurs, the contribution of the nonlinear part of the deformation potential becomes comparable to the linear part.

We shall concentrate on the effects of (a) a pure uniaxial tensile stress along the $\langle 111 \rangle$ direction, and (b) biaxial tensile stress in the (001) plane on the mobility of bulk Ge. The stress of type (a) introduces a longitudinal tensile strain, ε_l, along the $\langle 111 \rangle$ direction, and results in a transverse strain, $\varepsilon_t = -0.14 \varepsilon_l$.[12] The bulk results obtained in this way should also well describe nanowires wider than 10 nm.The effects of a $\langle 111 \rangle$ stress on nanowires have been discussed in Ref. 6 and we find very similar results for the band structure of the strained material. The stress of type (b) is composed of strains, $\varepsilon_{xx} = \varepsilon_{yy}$, in the (001) plane, and a transverse strain, $\varepsilon_{zz} = -0.76 \varepsilon_{xx}$, in the $\langle 001 \rangle$ direction. This type of strain would be obtained by the epitaxial growth of Ge on a substrate of a larger lattice constant, such as GeSnSi or InGaAs.

The acoustic phonon scattering has been obtained using the deformation potential approach.[10,13] The acoustic deformation potential, Ξ_Γ, was obtained using the frozen phonon approach of Ref. 10, and is in agreement with that found experimentally[11] at zero strain. The inter-valley phonon couplings were computed using the density functional perturbation theory approach,[10,14] from which the parameters for the L valley were extracted. Zhang *et al.*[6] report a nonlinear dependence of the Γ valley energy under shear strains. This will have an effect on the carrier scattering by phonons at the large values of strain needed to produce a direct bandgap. The linear shift of the Γ valley is described by the Ξ_Γ deformation potential. The nonlinear term in the energy shift, up to second order in the strain, is given by,

$$\begin{aligned} \delta E_2^\Gamma =& A\left(e_{xx}^2 + e_{yy}^2 + e_{zz}^2\right) \\ &+ B\left(e_{xx}e_{yy} + e_{xx}e_{zz} + e_{yy}e_{zz}\right) \\ &+ C\left(e_{xy}^2 + e_{yz}^2 + e_{zx}^2\right), \end{aligned} \quad (2)$$

where A, B, and C are the second order deformation potentials, and $e_{ii} = \varepsilon_{ii}$ and $e_{ij} = \varepsilon_{ij} + \varepsilon_{ji}$ are the Cartesian strain components. Following the approach of Ref. 10, the values of A, B, and C (see Table I) have been calculated using the frozen phonon approach, similarly to the calculation of Ξ_Γ.[15]

The variation of the inter-valley deformation potentials with strain was found to be negligible, except in the case of the L to L inter-valley deformation potential, $(D_t K)_{LL}$ (as defined in Ref. 11). However, this deformation potential is rather small, and its contribution to carrier scattering is

TABLE I. Intra- and inter-valley deformation potentials for the calculation of the electron-phonon scattering. Parameters for the L valley have been taken from Ref. 10. The inter-valley couplings are as defined in Ref. 11. The energies of the inter-valley and optical phonons are labeled $\hbar\omega_i$. The calculated lattice constant of Ge is $a_0 = 5.57$ Å. (The experimental value is $a_0 = 5.66$ Å.)

Ξ^Γ (eV)	− 5.3
Ξ_u^L (eV)	16.98
Ξ_d^L (eV)	− 6.27
A (eV)	20
B (eV)	152
C (eV)	− 72
$(D_t K)_{\Gamma L}$ (10^9 eV/m)	28.6
$(D_t K)_{LL}$ (10^9 eV/m)	7.9
$(D_t K)_{opL}$ (10^9 eV/m)	36.3
$\hbar\omega_{\Gamma L}$ (meV)	30
$\hbar\omega_{LL}$ (meV)	29
$\hbar\omega_{opL}$ (meV)	37
$\Delta E_1^{\langle 111 \rangle}(\varepsilon_l)$ (eV)	$0.838 - 12.6\varepsilon_l - 33.8\varepsilon_l^2$
$\Delta E_2^{\langle 111 \rangle}(\varepsilon_l)$ (eV)	$0.838 - 2.1\varepsilon_l - 66.2\varepsilon_l^2$
$\Delta E_1^{\text{biaxial}}(\varepsilon_{xx})$ (eV)	$0.838 - 27.7\varepsilon_{xx} + 122.0\varepsilon_{xx}^2$
$\Delta E_2^{\text{biaxial}}(\varepsilon_{xx})$ (eV)	$0.838 - 10.0\varepsilon_{xx} + 16.6\varepsilon_{xx}^2$

dwarfed by that of the acoustic phonons. The same is true for the scattering of optical phonons in the Γ valley: in the unstrained case it is forbidden by symmetry, and strain in the ⟨111⟩ direction increases it but imperceptibly, compared to acoustic phonon scattering. Likewise, the change of the *L*-valley effective mass with strain is of the order of 1% per percent of strain.

All of the calculations of the band structure have been performed using the GW approximation[16,17] with the ABINIT code.[18–20] We use the local density approximation (LDA) for exchange and correlation. Fritz Haber Institute (FHI) pseudopotentials (available in the ABINIT website[19]) are used for all calculations in this paper. We use an energy cut-off of 18 Hartree for the expansion of wavefunctions in all our calculations, except for those of the second order deformation potentials, which require a cut-off of 43 Hartree. The supercell sizes are the same as described in Ref. 10. The number of irreducible k-points is obtained using the 'kptrlen' capability of ABINIT. The required number of irreducible k-points for the first and second order deformation potentials is 134 and 198, respectively.

It is well known that the underestimate of the LDA direct bandgap, compared to experiment, gives rise to a corresponding underestimate of the effective mass, m_Γ, which can be understood simply in terms of $\mathbf{k}\cdot\mathbf{p}$ theory. In contrast, although the GW bandgap is typically close to the experimental value, it is difficult to directly calculate the effective mass using the GW method. Therefore, we have used the following simple, approximate scheme to estimate the strain-dependence of the band dispersion (and the effective mass) in the conduction band Γ valley: The direct bandgap for a given strain, ε, is determined using the GW method. The band dispersion is later calculated by a 5×5 matrix using the $\mathbf{k}\cdot\mathbf{p}$ theory,[21,22] accounting for strain and spin-orbit coupling.[23] Since we are only interested in the dispersion of the conduction band, we have neglected the matrix elements between the valence bands. We also considered the matrix element between the conduction band and valence bands to be given by free electron wavefunctions, with $P=2\pi\hbar/a_0$.[22] The only input needed by this model are the energy gaps (see below) and the spin-orbit coupling. This approximation gives an excellent fit to the LDA conduction band dispersion as a function of strain.

The conduction band dispersion is a function of its energy difference with all three highest valence bands, which are not degenerate under strain. The GW-calculated values as a function of strain are shown in Table I. In the strain cases considered here, the GW valence bands split into a singlet and a doublet (without spin-orbit). The energy gap between the conduction band at Γ (labeled as $\Gamma_{7,c}$ in Ref. 3), the valence band singlet ($\Gamma_{8,v1}$), and doublet ($\Gamma_{8,v2}$) are labeled ΔE_1^i and ΔE_2^i, respectively, where i is the type of strain. We note that as the bandgap closes, the energy becomes linear close to the band-edge.[24] The density of states of this nonparabolic dispersion, unlike that of a pure quadratic dispersion, does not vanish as the bandgap closes, which we find to be more realistic.

To simplify the mobility calculation, we have fitted the density of states and group velocity given by the $\mathbf{k}\cdot\mathbf{p}$ model, with third-order polynomials in energy and strain. The effective mass of the Γ valley in the unstrained system is found to be $m_\Gamma=0.04m_0$, which is in good agreement with the values reported by Refs.[11] and 3. The mobilities were then calculated[10] using the Boltzmann transport equation, in the relaxation time approximation, using only the first-principles calculated lattice and scattering parameters as input.

III. RESULTS

All of the calculated parameters are shown in Table I. Uniaxial ⟨111⟩ strain lifts the degeneracy of the *L* valleys, in agreement with Ref. 6, splitting them into a singlet (*L*1) along ⟨111⟩ and a triplet (*L*3) along $\langle\bar{1}11\rangle$, $\langle\bar{1}11\rangle$, and $\langle\bar{1}11\rangle$. Under positive strain, the *L*3 valleys are lowered in energy, which could potentially enhance the *n*-type carrier mobility by a few tenths of a percent due to the possibility of transport through a lower effective mass direction, albeit not in the ⟨111⟩ direction. Negative strain isolates the *L*1 valley, and the mobility could be enhanced if transport occurs along the direction transverse to the valley. However, if a larger tensile strain of $\varepsilon_{\langle111\rangle}=0.04$ is applied, the conduction Γ valley can be lowered below the *L*3 valleys. The smaller density of states of the Γ valley, together with the small acoustic deformation potential and lack of coupling to an optical phonon, results in a predicted room temperature mobility tens of times larger than that of unstrained Ge. A similar argument applies to biaxial strain. In this case, however, a much smaller strain of $\varepsilon_{xx}=\varepsilon_{yy}=0.015$ is required to lower the Γ valley below the *L* valleys. This means that the density of carriers in the Γ valley is potentially higher, resulting in much larger mobilities. The gaps close at $\varepsilon_{\langle111\rangle}=0.051$ and $\varepsilon_{xx}=0.03$, respectively.

In ⟨111⟩ stress, the nonlinear part of the deformation potential results in a decrease of the scattering of carriers by longitudinal acoustic phonons, but increases the hitherto negligible scattering by phonons from the transverse branch, increasing the total scattering overall. By this means, the total acoustic phonon scattering rate is increased by about 3.5 times at 4% strain. This increase in the scattering rate is counterbalanced by the reduction of the effective mass, yielding an overall increase in the carrier mobility. In the case of biaxial stress, the total scattering rate is reduced by half at $\varepsilon_{xx}=0.02$, and returns to its unstrained value at $\varepsilon_{xx}=0.07$. This nonlinear effect on the electron-phonon scattering accounts for the larger mobilities we obtain, compared to earlier estimates.[3]

Large strains are required to lower the Γ valley below *L*3. However, these strains have recently been proven to be well within the realizable limit in nanowires.[8,9] Therefore, we predict that the phonon-limited mobility of Ge can be enormously enhanced by applying positive stress in the ⟨111⟩ direction, as shown in Fig. 1. For example, an enhancement of five times the unstrained mobility is achievable if a positive strain of 4.7% is applied, while increasing the strain to 5% increases the mobility by 20 times the unstrained case.

We should note that the enhancement of the mobility is very sensitive to the strain configuration. The most desirable strain setting is that which most lowers the Γ valley below

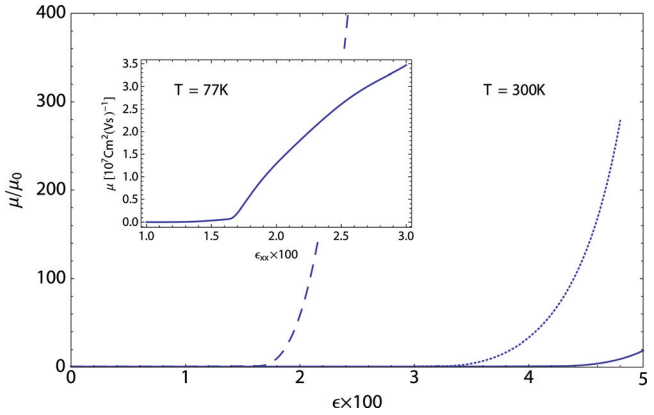

FIG. 1. (Color online) Room temperature mobility enhancement as a function of strain, for bulk Ge under a longitudinal stress that produces a strain, $\varepsilon = \varepsilon_{\langle 111\rangle}$, of up to 5%, and a transverse strain of $\varepsilon_t = -0.14\varepsilon_l$ (solid line); and for biaxially strained Ge in the x and y directions, with $\varepsilon = \varepsilon_{xx}$, ($\varepsilon_{xx} = \varepsilon_{yy}$), and a transverse strain, $\varepsilon_{zz} = -0.76\varepsilon_{xx}$ (dashed line). The dotted line shows the mobility enhancement for pure uniaxial $\langle 111\rangle$ strain, with $\varepsilon_t = 0$. The inset shows the phonon-limited mobility of biaxially (001) stressed Ge at a temperature of 77 K.

the L valley without closing the gap. For example, if the transverse strain due to relaxation were prevented, the enhancement of the mobility is predicted to be 3 orders of magnitude larger, since the strain required to lower the Γ below the L valley is reduced to $\varepsilon_l = 0.03$ (see the dotted curve in Fig. 1).

A more realistic possibility is the application of tensile bi-axial strain, as previously discussed.This case results in spectacular enhancements similar to the pure longitudinal $\langle 111\rangle$ strain, as shown by the dashed line of Fig. 1. This strain has been achieved by growing a narrow strip of Ge on a (001) $In_x Ga_{1-x}As$ alloy substrate.[7,25,26] The supplementary information of Ref. 6 (see reference within), and Ref. 5, in which the strains that produce a direct bandgap are shown, give a good indication of the potential candidates for the kind of strain required to achieve higher mobility.

In Fig. 1 (inset) we also show the low carrier concentration mobility of bi-axially (001) strained Ge at a temperature of 77 K. Due to the low effective mass, this low temperature mobility is one to two orders of magnitude larger than the corresponding theoretical estimate for GaAs.[27]

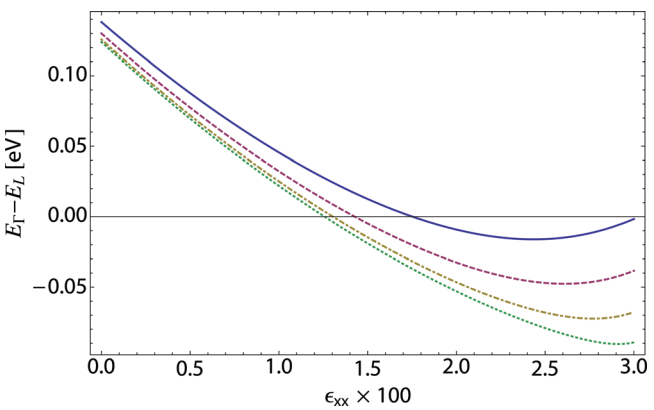

FIG. 2. (Color online) Energy difference between the confined Γ and L valleys as a function of bi-axial strain for a channel width = 20 nm (solid line), 30 nm (dashed line), 50 nm (dot-dashed line) and 100 nm (dotted line).

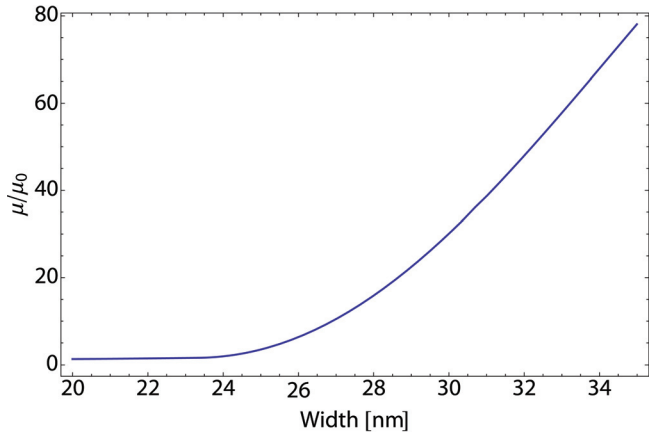

FIG. 3. (Color online) Maximum enhancement of the mobility in Ge as a function of channel width, for bi-axially strained Ge. The typical strain at which the maximum mobility enhancement is obtained is $\varepsilon_{xx} \approx 0.025$.

In effect, these large mobilities indicate that transport in strained Ge nanostructures will be ballistic in the absence of other scattering mechanisms such as interface roughness and impurity scattering. In practice, the latter are likely to dominate the carrier mobility, however, the inelastic mean free paths are expected to be extremely large. The decreased density of states, however, ensures that all types of scattering will have a small effect on the overall mobility.

These spectacular mobility enhancements in strained Ge ultimately disappear if the channel width is sufficiently small and quantum confinement raises the Γ valley (which has a small effective mass) above the L valley. The mobility enhancement only occurs if the carriers are predominantly in the Γ valley. Quantum confinement effects raise the Γ valley more than the L valley and compete with the effects of strain, which lower the Γ valley relative to the L valley. Thus, for a given channel width, there is an optimum strain to obtain maximum carrier mobility (see Fig. 2). A positive effect of confinement is that it decreases the rate at which the bandgap closes with strain. Assuming the case of highest confinement, that of a quantum well with infinite potential walls, Fig. 3 shows the resulting maximum mobility enhancement over unstrained Ge to be obtained at each channel width, starting at 4× with a 20 nm bi-axially strained channel. The values of the strain at which this occurs in the range shown are typically $\varepsilon_{xx} \approx 0.025$ (see Fig. 2). For a $\langle 111\rangle$ stressed wire, the mobility enhancements are much less dramatic, achieving a tenfold increase in mobility at 90 nm in diameter.

We must note that the calculated lattice constant of Ge is 5.57 Å, which is about 1.6% smaller than the experimental 5.66 Å. Using the experimental rather than the calculated lattice parameter would lower the energy of the Γ valley with respect to the L valley in the unstrained case, also reducing its effective mass, and therefore increasing the mobility enhancements observed in this work for the strained case.

IV. CONCLUSION

In summary, we have shown that the room temperature mobility of highly tensile bi-axially (001) strained Ge could

be increased several hundred times, and over a thousand times that of Si, in epitaxial thin Ge (001) films with strain, $\varepsilon_{xx} > 0.02$. The mobility of strained $\langle 111 \rangle$ grown Ge nanowires could be enhanced by 5–20 times if a uniaxial stress in the direction of growth is applied. Despite the competing effects of quantum confinement, these enhancements are sustainable in nanostructures of width of at least 20 nm. The low temperature mobilities are found to be over an order of magnitude higher than that of GaAs. The resulting ultrahigh mobilities make highly-strained Ge a very exciting candidate for CMOS channels and ultra-fast MOSFETs within the established Si-fabrication technology processes. Since the strains at which this is predicted to occur have already been demonstrated[7–9] in nanostructures, these extraordinary increases in mobility are well within the reach of the current technology.

ACKNOWLEDGMENTS

This work has been supported by Science Foundation Ireland.

[1]S. Takagi, T. Tezuka, T. Irisawa, S. Nakaharai, T. Numata, K. Usuda, N. Sugiyama, M. Shichijo, R. Nakane, and S. Sugahara, Solid-State Electron. **51**, 526 (2007).
[2]J. Liu, L. Kimerling, J. Michel, X. Sun, and R. Camacho-Aguilera, Opt.-Lett. **35**, 679 (2010).
[3]M. Fischetti and S. Laux, J. Appl. Phys. **80**, 2234 (1996).
[4]J. D. Sau and M. L. Cohen, Phys. Rev. B **75**, 045208 (2007).
[5]Y. Hoshina, K. Iwasaki, A. Yamada, and M. Konagai, Jpn. J. Appl. Phys. **48**, 04C125 (2009).
[6]F. Zhang, V. H. Crespi, and P. Zhang, Phys. Rev. Lett. **102**, 156401 (2009).
[7]N. Pavarelli, T. J. Ochalski, Y. Huo, G. Huyet, and J. S. Harris, Presentation at Photonics Europe (2010).
[8]D. Smith, V. Holmberg, and B. Korgel, ACS Nano **4**, 2356 (2010).
[9]L. Ngo, D. Almécija, J. Sader, B. Daly, N. Petkov, J. Holmes, D. Erts, and J. Boland, Nano Lett. **6**, 2964 (2006).
[10]F. Murphy-Armando and S. Fahy, Phys. Rev. B **78**, 035202 (2008).
[11]C. Jacoboni and L. Reggiani, Rev. Mod. Phys. **55**, 645 (1983).
[12]Obtained from density functional theory calculations.
[13]C. Herring and E. Vogt, Phys. Rev. **101**, 944 (1956).
[14]X. Gonze and C. Lee, Phys. Rev. B **55**, 10355 (1997).
[15]F. Murphy-Armando and S. Fahy (2011) (to be published).
[16]M. S. Hybertsen and S. G. Louie, Phys. Rev. B **34**, 5390 (1986).
[17]We have kept the zeroth order term of the GW approximation. In the LDA calculation, we impose zero temperature semiconductor filling of the bands. This ensures that the LDA wavefunctions are a good approximation to the quasiparticle wavefunctions.
[18]X. Gonze, B. Amadon, P.-M. Anglade, J.-M. Beuken, F. Bottin, P. Boulanger, F. B. Caliste, D. Caliste, R. Caracas, M. Cote, T. Deutsch, L. Genovese, P. Ghosez, M. Giantomassi, S. Goedecker, D. Hamann, P. Hermet, F. Jollet, G. Jomard, S. Leroux, M. Mancini, S. Mazevet, M. Oliveira, G. Onida, Y. Pouillon, T. Rangel, G.-M. Rignanese, D. Sangalli, R. Shaltaf, M. Torrent, M. Verstraete, G. Zerah, and J. Zwanziger, Computer Phys. Commun. **180**, 2582 (2009) (URL http://www.abinit.org).
[19]X. Gonze, G.-M. Rignanese, M. Verstraete, J.-M. Beuken, Y. Pouillon, R. Caracas, F. Jollet, M. Torrent, G. Zerah, M. Mikami, P. Ghosez, M. Veithen, J.-Y. Raty, V. Olevano, F. Bruneval, L. Reining, R. Godby, G. Onida, D. Hamann, and D. Allan, Z Kristallogr. **220**, 558 (2005).
[20]The ABINIT code is a common project of the Université Catholique de Louvain, Corning Incorporated, and other contributors (http://www.abinit.org).
[21]M. Cardona and M. H. Pollak, Phys. Rev. **142**, 530 (1965).
[22]P. Yu and M. Cardona, *Fundamentals of Semiconductors* (Springer, Berlin, 2001) pp. 121–136.
[23]S. Joyce, F. Murphy-Armando, and S. Fahy, Phys. Rev. B **75**, 155201 (2007).
[24]E. O. Kane, J. Phys. Chem. Solids **1**, 249 (1957).
[25]J. Menéndez and J. Kouvetakis, Appl. Phys. Lett. **85**, 1175 (2004).
[26]Y. Hoshina, A. Yamada, and M. Konagai, Jpn. J. Appl. Phys. **48**, 111102 (2009).
[27]C. M. Woue, G. E. Stillman, and W. T. Lindey, J. App. Phys **41**, 3088 (1970).